SPEKTRA: Jurnal Fisika dan Aplikasinya
Volume 8, Issue 2, August 2023
Homepage: doi.org/10.21009/SPEKTRA

DOI: doi.org/10.21009/SPEKTRA.082.03

EXPERIMENTAL AND COMPUTATIONAL STUDY OF NITROGEN-DOPED TiO_2 AS A PHOTOELECTRODE

Sitti Ahmiatri Saptari[1,*], Elvan Yuniarti[1], Lamin Rene Loua[2]

[1]*Prodi Fisika, FST, UIN Syarif Hidayatullah Jakarta, Indonesia*
[2]*Researcher, EcoSolutions Research Group, The Gambia*

*Corresponding Author Email: sitti.ahmiatri@uinjkt.ac.id

Received: 18 July 2023
Revised: 22 August 2023
Accepted: 24 August 2023
Online: 25 August 2023
Published: 30 August 2023

SPEKTRA: Jurnal Fisika dan Aplikasinya
p-ISSN: 2541-3384
e-ISSN: 2541-3392

ABSTRACT

TiO_2 has been widely used as a dye-sensitized solar cell (DSSC) photoelectrode, and attempts have been made to improve the performance of the photoelectrode by adding doping. This study aims to synthesize nitrogen (N) doped TiO_2 as a photoelectrode. The research was carried out experimentally and computationally using X-Ray Diffraction (XRD) test equipment, Fourier Transform Infra-Red (FTIR), and quantum espresso software using the Density Functional Theory (DFT) method. XRD results showed that TiO_2 has an anatase phase, and variations in the addition of nitrogen (doped N) of 10% w/w, 20% w/w, and 30% w/w did not produce a phase change. The FTIR results of N-doped TiO_2 and TiO_2 provide information on the functional groups of the samples. The wave number absorption area 1626 cm^{-1} indicates the presence of N-H bonds with a bending vibration mode. In addition, it can be seen that there is an N-H bond with a stretching vibration mode at wave number 3436 cm^{-1}. Computational calculations searched the band gap energy of each variation of N doping, and each obtained was 3.2 eV; 2.54 eV; 2.35 eV; and 1.64 eV. The results of this study indicate that the N-doped TiO_2 photoelectrode is expected to produce better DSSC efficiency because the addition of N-doped to TiO_2 causes a decrease in the bandgap energy. The N doping effect causes a new energy level. The new energy level must be positioned close to the existing valence and conduction bands. As a result, the energy required for electrons to transition from the valence band to the conduction band is reduced, effectively reducing the energy gap between the two. This change in

electronic structure facilitates more effortless movement of electrons, driving increased conductivity.

Keywords: TiO_2, N doping, photoelectrode, computing

INTRODUCTION

TiO_2 has been widely used as a DSSC photoelectrode, and attempts have been made to improve the performance of the photoelectrode by adding doping. This study aims to synthesize nitrogen (N) doped TiO_2 as a photoelectrode. The research was carried out experimentally and computationally using X-Ray Diffraction (XRD) test equipment, Fourier Transform Infra-Red (FTIR), and quantum espresso software using the Density Functional Theory (DFT) method. XRD results showed that TiO_2 has an anatase phase, and variations in the addition of nitrogen (doped N) of 10% w/w, 20% w/w, and 30% w/w did not produce a phase change. The FTIR results of N-doped TiO_2 and TiO_2 provide information on the functional groups of the samples. The wave number absorption area 1626 cm-1 indicates that Titanium dioxide is a material that's widely used and studied due to its attractive properties, and this can be seen in areas where it is used as a photocatalyst, photovoltaic, electronic device, anti-bacterial, and in cosmetic [1-5]. It is a naturally occurring oxide of titanium found in the family of transition metal oxides and exists in three crystalline forms; anatase, brookite, and rutile phase[6]. Among its many usages, as mentioned earlier, is being used in photovoltaics and photo-electrochromic, which are tired or categorized as 'energy' uses. The utilization of TiO_2 in photovoltaic is as a photoelectrode device as TiO_2 semiconductor material can absorb photons and transfer electrons. This process can generate current due to the formation of pairs of electrons and holes. This event creates pairs of electrons and holes [7]. However, from previous studies, pure TiO_2 has been absorbed in the ultraviolet region, and as such, to expand the absorption range of TiO_2, a sensitizer in the form of a dye is usually added to absorb visible light wavelengths [8]. The photoelectrode (s) must have a wide surface to attach the sensitizer to its surface [9]. The photoelectrode should also have a conduction and valence band energy that matches the HOMO LUMO on the sensitizer [10].

Various attempts have been made to match the TiO_2 gap energy level with a sensitizer. Various attempts have been made to improve the performance of TiO_2 so that it has a broad absorption wavelength range and can reduce the energy gap. These efforts include the synthesis of TiO_2 with the addition of Cu, Co, Ni, Cr, Mn, Fe, Ru, Au, Ag, Pt, and lanthanide groups [11]; another process is a high-energy ball mill. This process serves to reduce the crystal size of TiO_2 from 32 nm TiO_2 to 8 nm [12]. This article discusses the effect of adding urea as N doping. This study aimed to synthesize N-doped TiO_2 (N/TiO_2) and determine the geometric structure, electronic properties both experimentally and computationally.

Research on N-doped TiO_2 has been carried out experimentally and computationally using the DFT method by other researchers [13,14]. The difference with previous studies is the percentage (W/W) addition of urea experimentally. Computationally, the geometric structure model of the unit cell with the variation of N doping used differs from the model studied. This study used the sol-gel method, widely used in manufacturing TiO_2 with bulk samples studied

experimentally and computationally. We also focus on the crystal phase of anatase TiO_2 with a tetragonal crystal structure. The effect of adding N doping was investigated based on crystal size and computational calculations using a unit cell sample consisting of 12 atoms with a different model from previous researchers.

METHOD

In this study, experimental and computational methods were carried out. The experimental method synthesized undoped TiO_2 and TiO_2 doped with urea ($N/T.O_2$). The computational method used the Density Functional Theory (DFT) method.

Tools and materials

The tools used in this study were an analytical balance, 100 ml measuring cup, magnetic stirrer, oven, XRD, and FTIR. The materials used are TiO_2 bulk pro analysis, distilled water, and urea.

Experimental Method

This research begins with the synthesis of TiO_2 without doping. Synthesis was done by dissolving TiO_2 with 50 ml of distilled water and stirring using a magnetic stirrer for 2 hours at room temperature. The solution was precipitated for 24 hours and separated between the solid and liquid phases. Furthermore, the drying process of TiO_2 solids was carried out using an oven at 200^{o}C for 2 hours [15]. Furthermore, to obtain doped TiO_2, it was carried out in the same way, but each TiO_2 solution was added with a variation of urea. The TiO_2 samples prepared had variations in adding urea of 0, 10, 20, and 30% w/w FIGURE 1. Then the samples were tested by XRD (Shimadzu), and Fourier transforms infrared FTIR (Bruker) to determine their functional groups.

FIGURE 1. The TiO_2 samples prepared had variations in adding urea of (a)0%, (b)10%, (c)20%, and (d)30% w/w

Computational Method

The $_{TiO2}$ model used to simulate 0%, 10%, 20%, and 30% doped TiO_2 has a tetragonal geometric structure with a unit cell of 12 atoms. The 0% urea-doped TiO_2 model consists of 4 titanium atoms and eight oxygen atoms. TiO_2 doped with 10% urea is modeled simply by substituting one oxygen atom with one nitrogen atom (TiO_2-N). The 10% TiO_2-N model consists of 4 titanium atoms, seven oxygen atoms, and one nitrogen atom. The 20% urea-

doped TiO_2 atom model is modeled by replacing two oxygen atoms with two nitrogen atoms (TiO_2-2N). Next to model (TiO_2-3N) FIGURE 2.

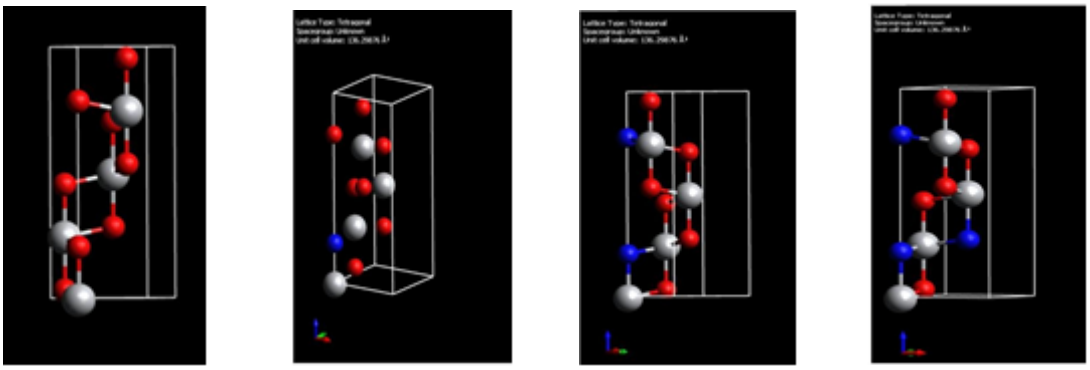

(a) (b) (c) (d)

FIGURE 2. Optimized TIO_2 structural model (a), optimized N-doped TIO_2 structural model (b), optimized 2N-doped TIO_2 structural model (c), optimized 3n-doped TIO_2 model (d) with red balls = oxygen atoms, gray balls = titanium atoms and blue balls = nitrogen atoms

In this study, modeling of nitrogen-doped TiO_2 was made using the Avogadro software, which was then optimized using the Density Functional Theory (DFT) + U8.5 method with the general gradient approach from Perdew-Burke-Ernzerhof (GGA+PBE) [16]. Calculations were performed using quantum espresso software. Furthermore, the results obtained by computation, namely density of state (DOS), gap energy, and diffraction pattern calculations, were obtained and visualized with Vesta software. Furthermore, the DFT method can calculate infrared spectra to determine the model's wavenumber and type of vibration.

RESULT AND DISCUSSION

This study discusses the TiO_2 diffraction patterns for doping variations from experimental and computational results, DOS calculation results and energy gap calculation results as well as experimental results of FTIR transmittance spectra in experiments.

TiO_2 Diffraction Pattern

The diffraction pattern of the TiO_2 sample with various nitrogen doping results from the XRD test experimentally can be seen in FIGURE 2, and the data is shown in TABLE 1. The diffraction pattern was matched to the ICDD database (International Center for Diffraction Data) reference number 00-021-1272. From these data, information was obtained that all samples had an anatase phase, meaning that variations in nitrogen doping of 10%, 20%, and 30% w/w on TiO_2 did not cause any phase changes [17]. However, TABLE 1 shows that the crystal size of the sample tends to decrease with increasing nitrogen doping. The decreased crystal size reinforces that Nitrogen doping of TiO_2 has been successfully carried out either by substitution (a nitrogen atom replaces the position of an oxygen atom) or by interstitial [18]. Nitrogen atoms are generally smaller, and their inclusion can cause distortions or strains within the lattice, resulting in smaller crystal sizes. The crystallite size (D) is usually determined through the Scherrer equation:

$$D = k\lambda/\beta\cos\theta \quad (1)$$

Where k is a shape factor that has a typical value between 0.89-0.94,λ is the X-ray wavelength, β is the full width at half maximum peak (in radians), and θ is the diffraction angle at which (1 0 1) intensity peaks appear [19]. The experimental and computational TiO_2 diffraction patterns have almost the same pattern (FIGURE 3, FIGURE 4).

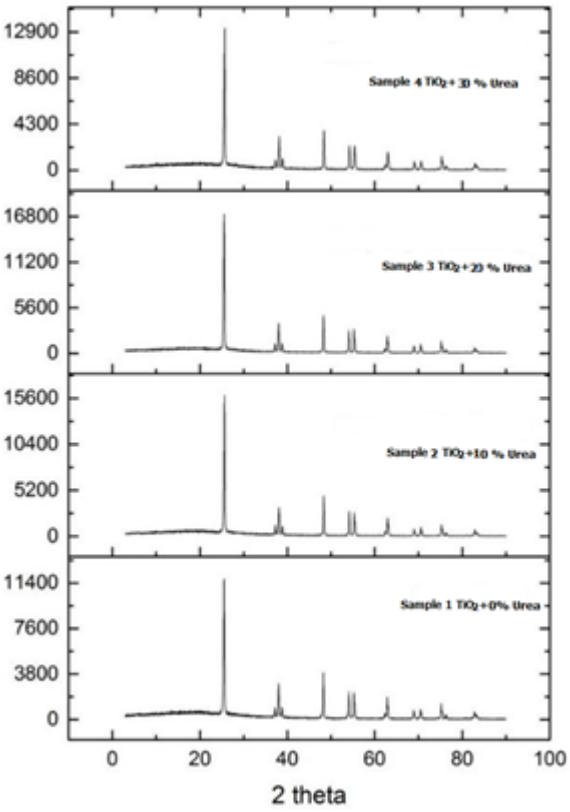

FIGURE 3. Experimental XRD pattern of 0%, 10%, 20%, 30% Nitrogen doped TiO_2 sample.

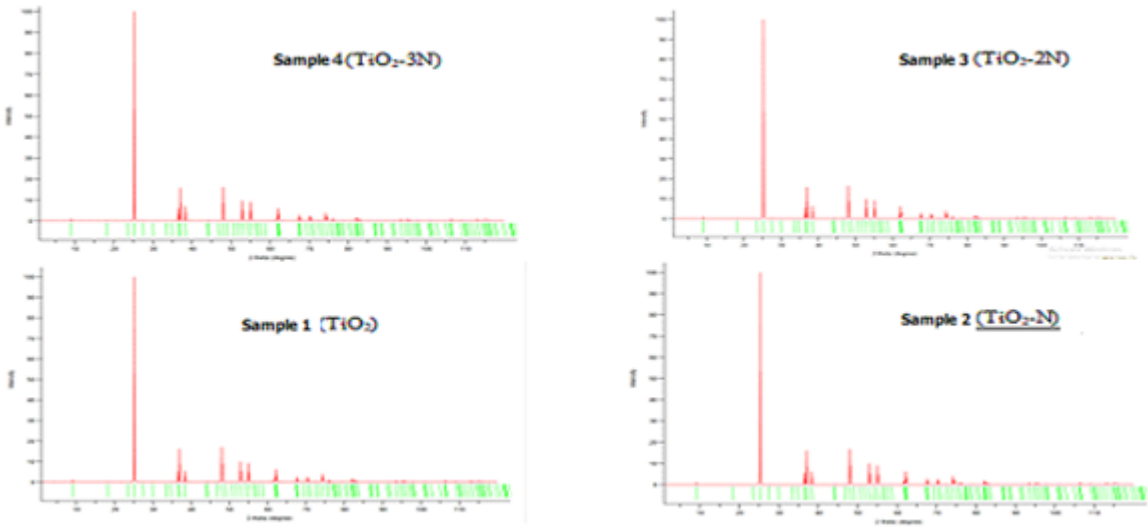

FIGURE 4. Computational xrd pattern of TiO_2 samples doped 0%,10%,20%,30% Nitrogen.

In the TiO_2 photoelectrode material with the addition of N doping, the figure of merit increase. Figure of merit is a thermoelectric parameter which usually indicates the material's ability to generate thermoelectric conversion efficiency. The figure of merit shows that the TiO_2 photoelectrode with the addition of doping experiences an increase in the efficiency of its thermoelectric properties. The figure of merit value can be seen in TABLE 1. Photo electrode TiO_2 by adding nitrogen can also be recommended as a thermoelectric material [20].

TABLE 1. XRD characterization data of TiO_2 samples with various nitrogen doping

Sample	2θ (der)	hkl	FWHM (der)	Crystal size (Å)	*Figure of merit*
TiO_2	25.51	101	0.174	382	0.544
	77.99	004	0.146		
	48.23	200	0.144		
TiO_2 + 10%urea	25.58	101	0.172	396	0.858
	38.07	004	0.174		
	48.30	200	0.148		
TiO_2 + 20%urea	25.54	101	0.196	364	0.551
	38.00	004	0.178		
	48.24	200	0.161		
TiO_2 + 30%urea	25.62	101	0.224	332	0.637
	38.11	004	0.221		
	48.33	200	0.218		

TiO_2 Geometry Structure

The optimization results of the TiO_2 model and the doped TiO_2 model can be seen in FIGURE 2. The models have lattice parameters a = b = 3.785 Å and c = 9.514 Å while α = β = ɣ= 90 degrees. The model shows that the crystal system of TiO_2 is tetragonal. This model was chosen for the calculation because it is by the experimental results obtained using the anatase phase. In addition, the unit cell is used, which is simple in calculations. Although the N-doped TiO_2 and TiO_2 models are simple, the calculation results can describe the experimental results. It can be shown that the calculation results are following the experimental results.

Density of State (*DOS*) TiO_2

The results (FIGURE 5) show that adding Nitrogen decreases the energy gap. The addition of Nitrogen also causes the growth of DOS in the state at 13 to 14 eV. Increasing the N doping causes an increase in DOS in that state. It is also seen that there is a shift in the upper edge of the valence band level towards higher energy. In addition, if the condition of the conduction band on the lower edge also decreases. The states at energies -17 and -18 eV have decreased DOS intensity with the addition of Nitrogen. Gab energy values based on calculations have the same values as experiments for TiO_2 without doping 3.2 eV.

The pattern of the addition of Nitrogen causes a decrease in the energy gap. This phenomenon is following previous experiments [18]. Effect doping Nitrogen The addition of Nitrogen in varying percentages reduces the energy gap due to a process known as nitrogen doping.

Reduces the energy gap happens because nitrogen atoms have different electronegativity compared to the atoms of the TiO_2 material being modified. When Nitrogen is incorporated into the TiO_2 material's structure, it creates new energy levels within the TiO_2 material's electronic band structure. These new energy levels are close to the existing valence and conduction bands. As a result, the energy required for electrons to transition from the valence band to the conduction band is decreased, effectively reducing the energy gap between them. This alteration in the electronic structure facilitates more effortless movement of electrons, promoting enhanced conductivity. Moreover, introducing Nitrogen can introduce defects or vacancies in the material's crystal lattice. These structural changes further contribute to the modifying [21]. Reducing the energy gap in DSSC photoelectrodes can improve their efficiency and performance. The energy gap is the difference between the highest filled energy level (valence band) and the lowest empty energy level (conduction band) in the photoelectrode material. The small energy gap means a broader range of incoming photons can be absorbed and generated to generate electron-hole pairs (excitons). The increased light absorption helps capture a more significant portion of the solar spectrum, which results in a higher photon-to-electron conversion efficiency[22]-promoting efficient charge separation, reducing energy losses, and enhancing overall cell performance. This optimization contributes to higher conversion efficiencies and reinforces the potential of DSSCs as a competitive technology in solar energy conversion [23].

TABLE 2: Functional Group TiO_2

Material	Energy Gap (eV)
TiO_2	3.2
TiO_2 doped N	2.54
TiO_2 doped 2N	2.35
TiO_2 doped 3N	1.64

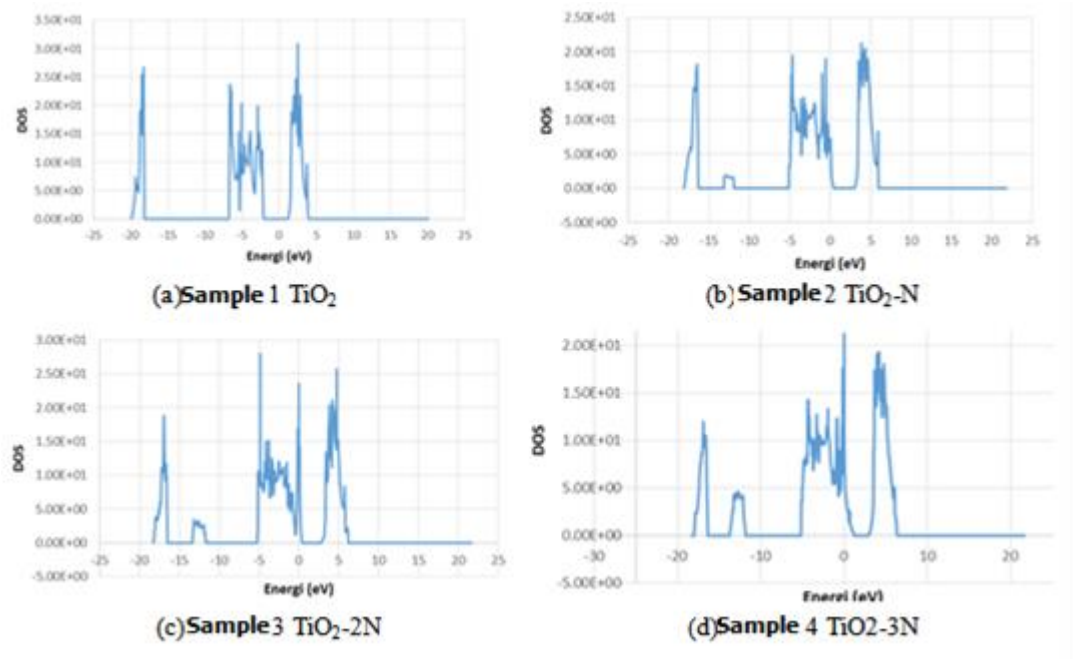

FIGURE 5. Density of state of TIO_2 and TIO_2 with various doping.

Infrared Spectra Analysis

The results of the FTIR test on the TiO_2 sample (FIGURE 6) show absorption at wave numbers 583-667 cm^{-1} as Ti-O stretching bonds and Ti-O stretching and O-Ti-O stretching. The wave number 1101 cm-^{1}, 1456 cm^{-1} and 1626 cm^{-1} indicate the presence of N atoms in the TiO_2 material. Another functional group is the Ti-OH bending mode at wave number 1635 cm^{-1}, indicating a bond for TiO_2 material and an O-H bonding vibration stretching mode at wave number 3427 cm^{-1} [8,24]. The wave numbers and functional groups of TiO_2 samples without doping can be seen in TABLE 3. In contrast, the functional groups with nitrogen doping experimentally can be seen in TABLE 4 and TABLE 5, showing the wave numbers that are owned computationally.

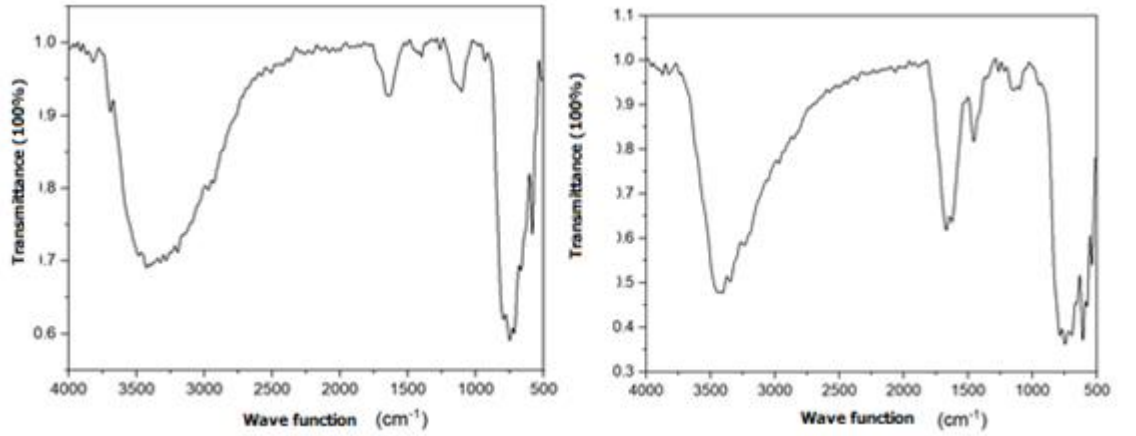

FIGURE 6. FTIR and TiO_2 spectra with various doping.

TABLE 3. FTIR Characterization Data from TiO_2 Experiment Results.

Wave Number (cm^{-1})	Functional Group
583	Ti-O streching
667-795	Ti-O streching and O-Ti-O streching
1104	C-O stretching
1635	Ti-OH bending
3427	O-H stretching

TABLE 4. FTIR Characterization Data from TiO_2 with Doped N Experiment Results.

Wave Number (cm^{-1})	Functional Group
538-609	Ti-N bond vibrations
696-788	Ti-O streching dan O-Ti-O streching
1101	
1456	
1626	Ti-OH *bending* / N-H *bending*
1670	C=C *stretching*
3436	N-H *stretching*

TABLE 5. Results Spectra Infra Red for TiO_2 and TiO_2 doped N

Frequency to	Peak Wave Number cm^{-1} (TiO_2)	Peak Wave Number cm-1 (N/TiO_2)
18	403.650686	289.713539
19	435.413913	299.181678
20	451.811685	407.39671
21	481.00187	417.172653
22	495.904194	433.773439
23	498.367414	468.779807
24	551.619773	483.029016
25	566.411119	494.653581
26	567.834721	516.07199
27	574.010794	563.303902
28	576.865037	571.088866
29	577.994188	577.388019
30	694.237541	586.495959
31	695.28559	597.154686
32	702.866546	615.66647
33	706.54744	702.443891
34	-	706.231464
35	-	732.916353
36	-	753.535075

CONCLUSION

This research has succeeded in synthesizing Nitrogen-doped TiO_2 with variations of 0%, 10%, 20%, and 30% w/w urea. The addition of Nitrogen doping to TiO_2 decreases the band gap energy, indicating that Nitrogen-doped TiO_2 is expected to increase the efficiency of DSSC. XRD's experimental and computational results have the same pattern for angle two theta. The pattern did not change with the addition of N doping. The size of TiO_2 crystals in the experiment decreased with the addition of doping. They have decreased the size of TiO_2 crystal. This occurs due to the substitution of oxygen atoms by Nitrogen. The experimental FTIR characterization results in the functional group reinforce these results. The wave number 538-609cm^{-1}, 1101 cm^{-1}, 1456 cm^{-1}, and 1626 cm^{-1} indicate the presence of N atoms in the TiO_2 material. The functional group calculation results are at wave number 403-706 cm^{-1}. In calculating the addition of doping is at wave number 289-753 cm^{-1}.

ACKNOWLEDGEMENT

Thank you to UIN Syarif Hidayatullah, especially the PUSLITPEN and LP2M institutions which have funded this research from BOPTN funds for the 2021 fiscal year. We also thank the Theory Lab of the Physics Department of IPB.

REFERENCES

[1] Nasikhudin *et al*., "Study on Photocatalytic Properties of TiO_2 Nanoparticle in various pH condition," *Journal of Physics: Conference Series*, vol. 1011, p. 012069, 2018.

[2] S. A. Mahmoud, B. S. Mohamed and H. M. Killa, "Synthesis of Different Sizes TiO_2 and Photovoltaic Performance in Dye-Sensitized Solar Cells," *Frontiers in Materials*, vol. 8, p. 714835, 2021.

[3] G. A. Illarionov *et al*., "Memristive TiO_2: Synthesis, Technologies and Applications," *Frontiers in Chemistry*, vol. 8, p. 724, 2020.

[4] E. Maryani *et al*., "The Effect of TiO_2 additives on the antibacterial properties (Escherichia coli and Staphylococcus aureus) of glaze on ceramic tiles," *IOP Conference Series: Materials Science and Engineering*, vol. 980, no. 1, p. 012011, 2020.

[5] S. Sharma *et al.*, "Fueling a hot debate on the application of TiO_2 nanoparticles in sunscreen," *Materials (Basel)*, vol. 12, no. 14, p. 2317, 2019.

[6] D. R. Eddy *et al*., "Heterophase Polymorph of TiO_2 (Anatase, Rutile, Brookite, TiO_2 (B)) for Efficient Photocatalyst: Fabrication and Activity," *Nanomaterials*, vol. 13, no. 4, p. 704, 2023.

[7] A. A. F. Husain *et al*., "A review of transparent solar photovoltaic technologies," *Renewable and sustainable energy reviews*, vol. 94, pp. 779-791, 2018.

[8] T. Fang *et al.*, "Effect of Germanium on the TiO_2 Photoanode for Dye Sensitized Solar Cell Applications. A Potential Sintering Aid," *IOP Conference Series: Materials Science and Engineering*, vol. 358, no. 1, p. 012015, 2018, doi: 10.1088/1757-899X/358/1/012015.

[9] M. F. Maulana *et al*., "Dye Sensitized Solar Cell (DSSC) Efficiency Derived from Natural Source," *Jurnal Fisika dan Aplikasinta*, vol. 17, no. 3, pp. 68-73, 2021.

[10] J. R. De Lile *et al*., "Do HOMO-LUMO energy levels and band gaps provide sufficient understanding of Dye-sensitizer activity trends for water purification?," *ACS Omega*, vol. 5, no. 25, pp. 15052-15062, 2020.

[11] H. Dong *et al*., "An overview on limitations of TiO_2-based particles for photocatalytic degradation of organic pollutants and the corresponding countermeasures," *Water Research*, vol. 79, pp. 128-146, 2015.

[12] G. Batdemberel *et al*., "Effect of High-Energy Vibrating Ball Milling in the Reduction of the Crystallite Size of TiO_2 Particles," *Journal of Materials Science and Chemical Engineering*, vol. 9, no. 11, pp. 7-14, 2021.

[13] S. A. Ansari, M. Khan and O. Ansari, "Nitrogen-doped titanium dioxide (N-doped TiO_2) for visible light photocatalysis," *New Journal of Chemistry*, vol. 40, no. 4, pp. 3000-3009, 2016.

[14] W. Navarra *et al*., "Density Functional Theory Study and Photocatalytic Activity of ZnO/N-Doped TiO_2 Heterojunctions," *The Journal of Physical Chemistry C*, vol. 126, no. 16, pp. 7000-7011, 2022.

[15] A. D. Rosanti, A. R. Wardani and E. U. Latifah, "Pengaruh Variasi Konsentrasi Urea Terhadap Fotoaktivitas Material Fotokatalis N/TiO_2 Untuk Penjernihan Limbah Batik Tenun Ikat Kediri," *Jurnal Kimia Riset*, vol. 5, no. 1, pp. 55-66, 2020.

[16] M. H. Samat *et al*., "Structural and electronic properties of TiO_2 polymorphs with effective on-site coulomb repulsion term: DFT+U approaches," *Materials Today: Proceedings*, vol. 17, pp. 472-483, 2019.

[17] P. V. Bakre, S. G. Tilve and R. N. Shirsat, "Influence of N sources on the photocatalytic activity of N-doped TiO_2," *Arabian Journal of Chemistry*, vol. 13, no. 11, pp. 7637-7651, 2020.

[18] S. Karim, P. Pardoyo and A. Subagio, "Sintesis dan Karakterisasi TiO2 Terdoping Nitrogen (N-Doped TiO_2) dengan Metode Sol–Gel," *Jurnal Kimia Sains Dan Aplikasi*, vol. 19, no. 2, pp. 63-67, 2016.

[19] J. Gomes *et al*., "N-TiO_2 photocatalysts: A review of their characteristics and capacity for emerging contaminants removal," *Water (Switzerland)*, vol. 11, no. 2, p. 373, 2019.

[20] H. Liu *et al*., "High-thermoelectric performance of TiO_{2-x} fabricated under high pressure at high temperatures," *Journal of Materiomics*, vol. 3, no. 4, pp. 286-292, 2017.

[21] H. J. Goldsmid, "Improving the thermoelectric figure of merit," *Science and Technology of Advanced Materials*, vol. 22, no. 1, pp. 280-284, 2021.

[22] O. I. Francis and A. Ikenna, "Review of Dye-Sensitized Solar Cell (DSSCs) Development," *Natural Science*, vol. 13, no. 12, pp. 496-509, 2021.

[23] Z. Xiang *et al*., "Improving energy conversion efficiency of dye-sensitized solar cells by modifying TiO_2 photoanodes with nitrogen-reduced graphene oxide," *ACS Sustainable Chemistry & Engineering*, vol. 2, no. 5, pp. 1234-1240, 2014.

[24] A. Romadhoni *et al*., "of TiO_2 -N as Filler in Polyethersulfone Membranes for Laundry Waste Treatment," *Jurnal Sains dan Seni ITS*, vol. 8, no. 2, pp. C7-C11, 2019.